

Environmental Effects of the Fukushima Daiichi Nuclear Power Plant Accident

Katsumi Hirose

Abstract A gigantic earthquake and resulting tsunami, occurred on March 11, 2011, causing the Fukushima Daiichi Nuclear Power Plant (FDNPP) accident. Large amounts of radionuclides emitted in the atmosphere (^{131}I : 160 PBq, ^{137}Cs : 15 PBq) and predominantly deposited on the Japanese Island and the western North Pacific, and a considerable part of them were dispersed in the Northern Hemisphere. After the accident, the Japanese Government started emergency monitoring of environmental radioactivity. Worldwide radioactivity measurements including CTBTO in the Northern Hemisphere had detected the Fukushima-derived radionuclides in the atmosphere. In this chapter, environmental radioactivity monitoring results in the early stage of the Fukushima accident are described.

Keywords Fukushima earthquake · Atmospheric radioactivity · Radioactivity contamination mapping · Ambient dose rate measurement

1 Introduction

On March 11, 2011, a big earthquake (The Great East Japan Earthquake), which was a moment magnitude of 9.0 with a hypocentral region about 500 km long and 200 km wide, attacked the northeast Honshu island, Japan. After the big earthquake, a gigantic tsunami hit east coast of the northeast Honshu island, whose wave height was more than 15 m. Just after the earthquake, fission reaction in all of reactors constructed in the northeast Honshu Island was safely stopped. The location of nuclear power plants and nuclear facilities in the northeast Honshu Island is shown in Fig. 1. However, gigantic tsunami in addition to the earthquake seriously damaged the electric system of the Fukushima Daiichi Nuclear Power Plant (FDNPP) (37.42°N, 141.03°E). As a result, there was break down in the cooling system of nuclear reactors in the FDNPP. This was a cause of meltdowns of nuclear fuels and

K. Hirose (✉)

Department of Materials and Life Sciences, Faculty of Science and Technology,
Sophia University, Tokyo, Japan
e-mail: hirose45037@mail2.accsnet.ne.jp

Geosphere Research Institute, Saitama University, Saitama, Japan

D. Sengupta (ed.), *Recent Trends in Modelling of Environmental Contaminants*,
DOI 10.1007/978-81-322-1783-1_7, © Springer India 2014

167

Fig. 1 Location of the FDNPP and several monitoring stations. The *red area* shows a rough area of the hypocentral region of “The Great East Japan Earthquake”. The *closed circle* shows nuclear power plant. The *open circle* shows environmental radioactivity monitoring station discussed in this chapter

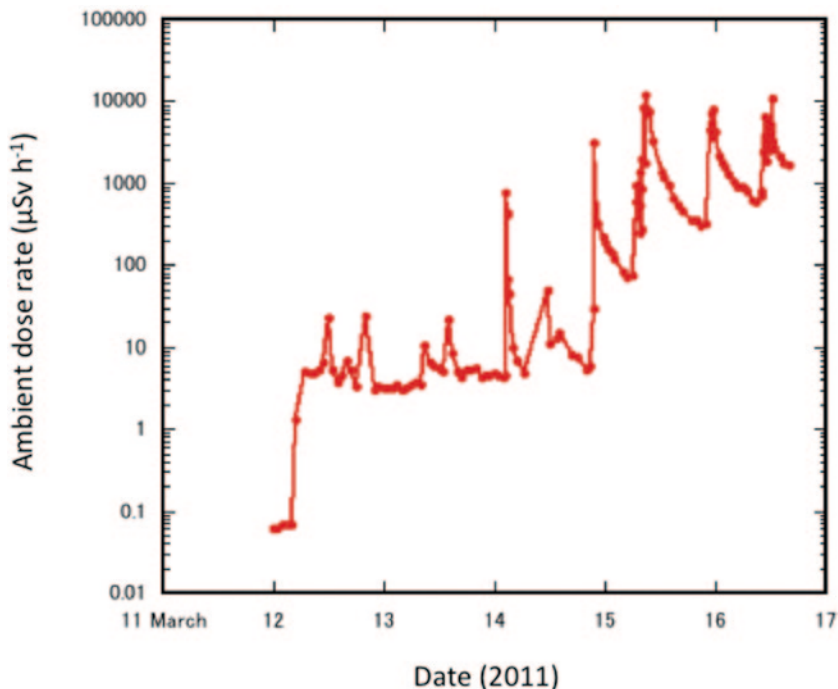
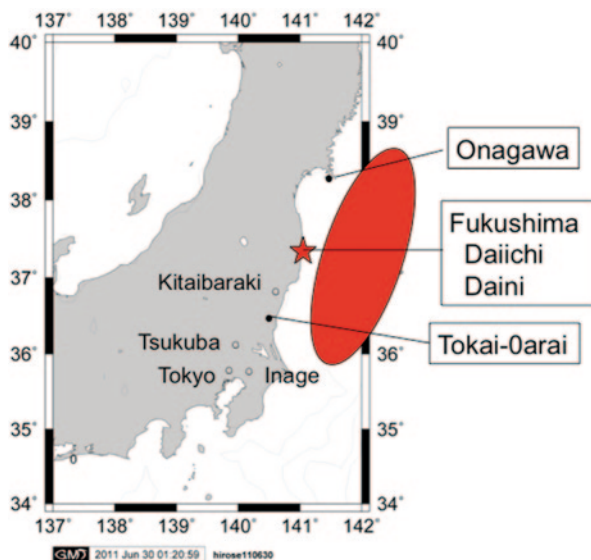


Fig. 2 Temporal change of ambient dose rate measured at the front gate of the FDNPP. This figure depicts data from TEPCO (2011). Peaks of the ambient dose rate almost corresponded to events such as explosions, vent, and others

resulting hydrogen explosions of No 1 Reactor and No 3 Reactor buildings in the FDNPP, which happened on March 12 and 14, respectively. In addition to explosions of nuclear reactors, an explosion occurred in the No 4 Reactor building on March 15, for which the sources of flammable gas are unknown because spent fuel in the No 4 reactor in spent fuel pool appeared to have been covered with water. An explosion occurred in the No 2 Reactor on March 15, suffered to lower suppression area (RJG 2011). On the early morning of March 12, ambient dose rate in the reactor site increased rapidly (Fig. 2), which means that atmospheric emission of radionuclides from the FDNPP was started as a result of meltdowns of nuclear fuel. On March 15–16, 2011, after the serious damage of the No. 2 Reactor (TEPCO 2011), the ambient dose rate at the FDNPP site showed pronounced peaks (Fig. 2), which implies occurrence of dominant radioactivity emissions. Especially, explosions of the FDNPP lead to serious radioactivity release in the atmosphere. However, exact emission history of the FDNPP-derived radionuclides in the atmosphere is the further study, although Chino et al. (2011) tried to reproduce the emission sequence of each radionuclide from the FDNPP.

Just after the accident, the Japanese Government and Prefectural Governments started emergency radioactivity monitoring to assess radiological and environmental effects of radioactivity emitted from the FDNPP accident (MEXT 2012). Preliminary airborne monitoring conducted by the US DOE (Lyons and Colton 2012) revealed that highly radioactive contamination area spread a narrow region from the FDNPP to about 60 km northwest region in the Fukushima Prefecture. The Ibaraki Prefectural Government has constructed a new monitoring system at sites (Kita-ibaraki and Takahagi) near Fukushima Prefecture. Temporal variations of the ambient dose rate observed at monitoring stations in Ibaraki Prefecture (Fig. 3) indicated that the radioactive plume first arrived in the Kanto Plain on March 15, 2011 (IPG 2011). On March 15–23, 2011, the effect of local fallout of the FDNPP-derived radionuclides spread over the Kanto Plain, which includes Tokyo and other major cities in the Kanto area. As did governmental monitoring, many research institutes and universities in Japan have measured FDNPP-derived radioactivity in environmental samples (Amano et al. 2012; Doi et al. 2013; Furuta et al. 2011; Kanai 2012). Furthermore, the Comprehensive Nuclear-Test-Ban Treaty (CTBTO) network (CTBTO, <http://www.ctbto.org/press-centre/highlights/2011/fukushima-related-measurements-by-the-ctbto/>) and regional monitoring stations in many countries have monitored the FDNPP-derived radioactivity in surface air and deposition.

In this chapter, monitoring results of atmospheric radioactivity derived from the FDNPP were summarized based on MEXT data (Chino et al. 2011) and published papers.

2 Total Atmospheric Release

The most important interest regarding nuclear reactor accidents is what kinds of radionuclides and what amount of each radionuclide was released in the environment. Japanese Government has conducted to estimate total atmospheric releases

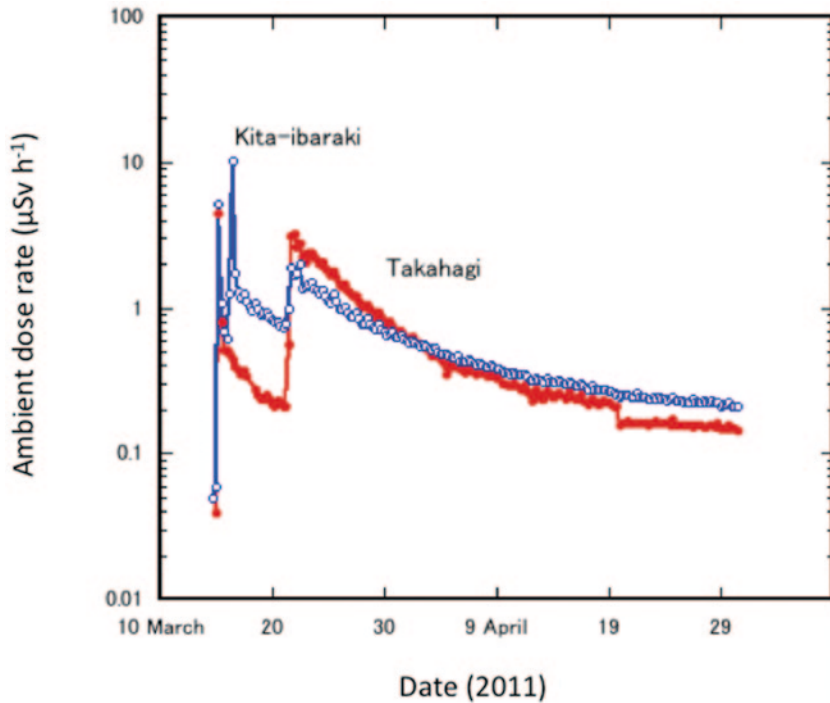


Fig. 3 Temporal variations of ambient dose rate observed in Ibaraki Prefecture. Data were cited by IPG (2011). Peaks on March 15 corresponded to the passage of radioactive plume. *Open circle*: Kita-ibaraki, *closed circle*: Takahagi

of radioactivity from the FDNPP based on the analysis of reactor status (RJG 2011); total atmospheric releases of ^{131}I and ^{137}Cs were 160 PBq and 15 PBq, respectively, which are about one order of magnitude less than the Chernobyl accident (IAEA 1986; UNSCEAR 2000). The total release of each radionuclide from the FDNPP is shown in Table 1. On the other hand, based on the inverse modeling method using monitoring data, Chino et al. (2011) estimated 150 PBq ($=10^{15}$ Bq) of ^{131}I and 12 PBq of ^{137}Cs as the total atmospheric releases of radioactivity from the FDNPP. Stohl et al. (2011) estimated 16.7 EBq ($=10^{18}$ Bq) of ^{133}Xe and 35.8 PBq of ^{137}Cs as the total atmospheric releases of radioactivity from the FDNPP, in which the ^{133}Xe emission is the largest radioactive noble gas release in the radioactivity emission history not associated with nuclear-weapons testing. There was no significant difference of the total release of ^{133}Xe between estimation methodologies, because all ^{133}Xe inventory, at cease of nuclear fission in three nuclear reactors of the FDNPP, was emitted in the atmosphere. On the other hand, there is rather large difference in total ^{137}Cs release between estimation methodologies. One of major causes is that monitoring data was limited in several stations of land area, although in the initial stage of the FDNPP accident the radioactive plume flowed toward ocean

Table 1 Radionuclides released from the FDNPP and total emission amount of each radionuclide. (RJG 2011)

Radionuclide	Half-life	Reactor I	Reactor II	Reactor III	Total release
		PBq	PBq	PBq	PBq
Xe-133	5.2 d	3,400	3,500	4,400	11,000
Cs-134	2.06 y	0.71	16	0.82	18
Cs-137	30.0 y	0.59	14	0.71	15
Sr-89	50.5 d	0.082	0.68	1.2	2
Sr-90	29.1 y	0.0061	0.048	0.085	0.14
Ba-140	12.7 d	0.13	1.1	1.9	3.2
Te-127m	109 d	0.25	0.77	0.069	1.1
Te-129m	33.6 d	0.72	2.4	0.21	3.3
Te-131m	30.0 h	2.2	2.3	0.45	5
Te-132	78.2 h	25	57	6.4	88
I-131	8.02 d	12	140	7	160
I-132	2.30 h	0.013		0.000037	0.013
I-133	20.8 h	12	26	4.2	42
I-135	6.57 h	2	0.074	0.19	2.3
Sb-127	3.85 d	1.7	4.2	0.45	6.4
Sb-129	4.3 h	0.14	5.6E ⁻⁵	0.0023	0.14
		TBq	TBq	TBq	TBq
Ru-103	39.3 d	0.0025	0.0018	0.0032	0.0075
Ru-106	368 d	0.00074	0.00051	0.00089	0.0021
Zr-95	64.0 d	0.46	16	0.22	17
Ce-141	32.5 d	0.46	17	0.22	18
Ce-144	284 d	0.31	11	0.14	11
Np-239	2.36 d	3.7	71	1.4	76
Pu-238	87.7 y	0.00058	0.018	0.00025	0.019
Pu-239	24,065 y	0.000086	0.0031	0.00004	0.0032
Pu-240	6,537 y	0.000088	0.003	0.00004	0.0032
Pu-241	14.4 y	0.035	1.2	0.016	1.2
Y-91	58.5 d	0.31	2.7	0.44	3.4
Pr-143	13.6 d	0.36	3.2	0.52	4.1
Nd-147	11.0 d	0.15	1.3	0.22	1.6
Cm-242	162 d	0.011	0.077	0.014	0.1
Mo-99	66.0 h	0.0026	0.0012	0.0029	0.0067

side (Takemura et al. 2011). Aoyama et al. (2012) estimated 10.5 ± 2.5 PBq as the total amount of atmospheric ^{137}Cs input in the North Pacific, based on radiocesium (^{137}Cs , ^{134}Cs) data in the North Pacific waters. In order to improve estimation of the total released radionuclides from the FDNPP, it is necessary to have information about more precious monitoring data, as did physical and chemical properties of released radionuclides.

3 Surface Air Monitoring

Radioactivity measurement in surface air is one of the most important issues in emergency environmental monitoring. The Japanese Government, including Prefectural Governments and Tokyo Electric Power Co. (TEPCO), started measurements of radioactivity in surface air using monitoring car as an emergency monitoring (TEPCO 2011; MEXT 2012). However, continuous sampling of air from both accidental reactor sites and areas from 20 to 60 km of the FDNPP has not been conducted. On the other hand, some research institutes (Amano et al. 2012; Doi et al. 2013; Furuta et al. 2011; Kanai 2012) and universities (Momoshima et al. 2012) in Japan have carried out continuous surface air sampling and have measured radioactivity in surface air samples. They had detected the FDNPP-derived radionuclides since late March 2011 in surface air samples. Air monitoring results reveal that dominant detected radionuclides originating from the FDNPP were radioactive noble gases (^{133}Xe , $^{131\text{m}}\text{Xe}$, $^{133\text{m}}\text{Xe}$, ^{135}Xe), radioiodine (^{132}I , ^{131}I), and radiocesium (^{134}Cs , ^{136}Cs , ^{137}Cs), although detected radionuclides in airborne particles were ^{133}I , ^{132}I , ^{131}I , ^{134}Cs , ^{136}Cs , ^{137}Cs , ^{132}Te , $^{129\text{m}}\text{Te}$ (^{129}Te), ^{99}Mo ($^{99\text{m}}\text{Tc}$), ^{140}Ba (^{140}La), and $^{110\text{m}}\text{Ag}$ (Amano et al. 2012; Furuta et al. 2011; Yonezawa and Yamamoto 2011). In contrast to the Chernobyl accident, significant amounts of refractory fission products such as ^{106}Ru , ^{103}Ru , and ^{95}Zr have not been detected in environmental samples for the FDNPP accident. Surface air measurements documented that radioactive plume first arrived in the Kanto Plain on March 15, 2011, which coincided with abrupt increase of the ambient dose rate (Fig. 3). After that, the FDNPP-derived radionuclides were transported in the northern hemisphere in late March and April 2011; ^{131}I and ^{137}Cs were detected in the Asia (Bolsunovsky and Dementyev 2011), North America (Bowyer et al. 2011; Zhang et al. 2011), Europe (Lozano et al. 2011; Pittauerová et al. 2011), and Arctic (Paatero et al. 2012).

3.1 Regional and Local Monitoring

Short-lived radioiodine (^{131}I , ^{132}I , and ^{133}I) within the FDNPP-derived radionuclides is an important radionuclide to monitor in early stage of nuclear reactor accidents because of higher health risk to radiation dose due to inhalation. However, there is limited information on short-lived radioiodine concentrations in surface air including gaseous and particulate forms; in the sites near Fukushima, gaseous ^{131}I have been reported at Inage, Chiba (Amano et al. 2012) and Oarai, Ibaraki (Furuta et al. 2011). Although Kanai (2012) reported ^{131}I concentrations in aerosols at Tsukuba, there was no information on early stage data in March 2011 and gaseous ^{131}I . The gaseous ^{131}I is conventionally defined as radionuclides adsorbed onto activated carbon fiber filter.

The temporal variation of the total ^{131}I concentrations (total gas plus particulate) at Oarai (about 100 km south of the FDNPP) and Tsukuba (about 170 km of the FDNPP) is shown in Fig. 4. The first peak of ^{131}I , being the highest concentrations

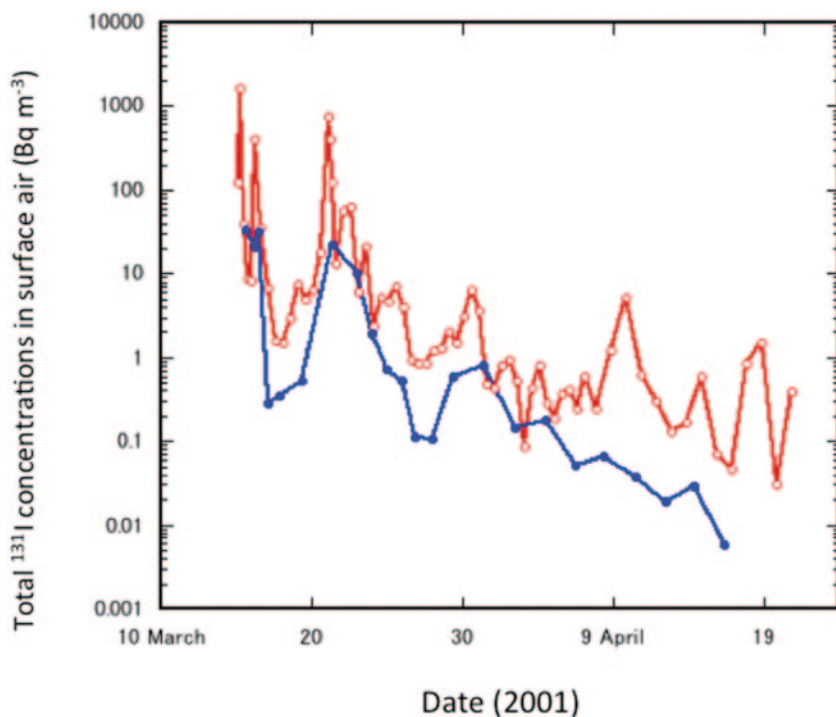


Fig. 4 Temporal variations of total ¹³¹I concentrations in surface air observed at Oarai (*open circle*) and Tsukuba (*closed circle*). This figure depicts the data cited from Doi et al. (2012) and Furuta et al. (2011)

at Tsukuba (33 Bq m^{-3} (8 h mean value)) and Oarai ($1.4 \times 10^3 \text{ Bq m}^{-3}$ (3 h mean value)) during the observation period, respectively, occurred on March 15–16, 2011, which coincided with maximum of the ambient dose rate of the corresponding site. On March 15–16, 2011, the high ¹³¹I concentrations in surface air were observed in Setagaya (Tokyo) (about 240 km of the FDNPP) and Inage (about 220 km of the FDNPP), where the ¹³¹I concentrations in surface air were $2.4 \times 10^2 \text{ Bq m}^{-3}$ (1 h mean value) and 33 Bq m^{-3} (27 h mean value) (Amano et al. 2012), respectively. The ¹³¹I concentrations in surface air at four sites decreased with distance from the FDNPP. The second peak of total ¹³¹I at Tsukuba (Doi et al. 2013) and Oarai (Furuta et al. 2011) appeared on March 20–22, which also coincided with the second peak of ambient dose rate at the corresponding sites. A similar peak of ¹³¹I was observed in Setagaya and Inage on March 20–22. The total ¹³¹I concentration in surface air at Tsukuba, which showed some peaks corresponding to periods of March 30 to April 1, April 17–19, and May 5–7, decreased as an apparent half life of 2.7 days (Doi et al. 2013), and it is difficult to detect ¹³¹I in air samples of the Kanto Plain in June, 2011 (detection limit: 0.1 mBq m^{-3}).

In order to have better understanding of the atmospheric behaviors of ¹³¹I, the temporal variation of gaseous ¹³¹I/total ¹³¹I ratio observed at Tsukuba was examined,

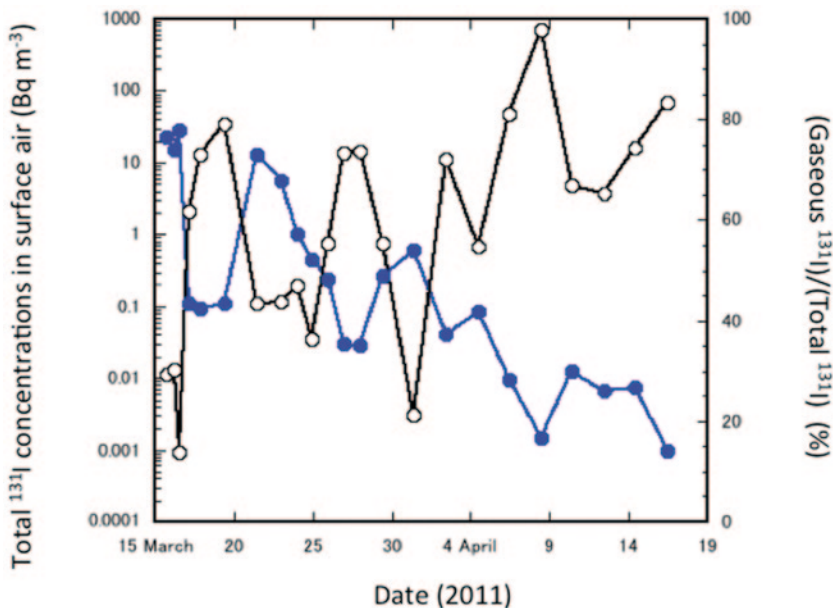


Fig. 5. Temporal variation of percentage of gaseous ^{131}I to total ^{131}I observed at Tsukuba. *Open circle* and *closed circle* show the percentage of gaseous ^{131}I to total ^{131}I and the concentration of total ^{131}I , respectively. This figure depicts the data cited from Doi et al. (2013)

in which the gaseous radioiodine (^{131}I , ^{133}I) was captured with the activated carbon fiber filter (Doi et al. 2013). The result is shown in Fig. 5. A lower portion of the gaseous ^{131}I almost corresponded to a peak of the total ^{131}I concentration in surface air; the lowest percentage of the gaseous ^{131}I to the total ^{131}I (13%) appeared in occurrence of the highest total ^{131}I concentration on March 16, 2011. The percentage of the gaseous ^{131}I to the total ^{131}I in each peak increased with time. The similar trend of increasing percentage of the gaseous ^{131}I was observed at Oarai (Furuta et al. 2011). These findings suggest that, as a possible process, the gaseous ^{131}I remained in the atmosphere longer than the particulate ^{131}I , and, as another possible process, the gaseous ^{131}I was preferentially emitted into atmosphere comparing with the particulate ^{131}I due to change of the radioactivity-released conditions in the accidental reactors such as decline of temperature. Other possible cause of increasing gaseous ^{131}I may be volatilization of deposited ^{131}I due to biological processes (Amachi et al. 2011; Muramatsu, and Yoshida 1995).

^{133}I was detected in surface air samples collected at Oarai, Tsukuba, and Inage as did ^{131}I , on March 15, 2011 (Amano et al. 2012; Doi et al. 2013; Furuta et al. 2011; Kanai 2012). The maximum concentrations of ^{133}I in surface air at Oarai, Tsukuba, and Inage on March 15, 2011 were 18, 2.6, and 1.9 Bq m^{-3} , respectively. The ^{133}I concentrations in surface air rapidly decreased and ^{133}I could not be detected in the end of March 2011. The temporal change of $^{133}\text{I}/^{131}\text{I}$ ratio in surface air at each site, which was 0.1 on March 15, 2011, decreased exponentially as shown

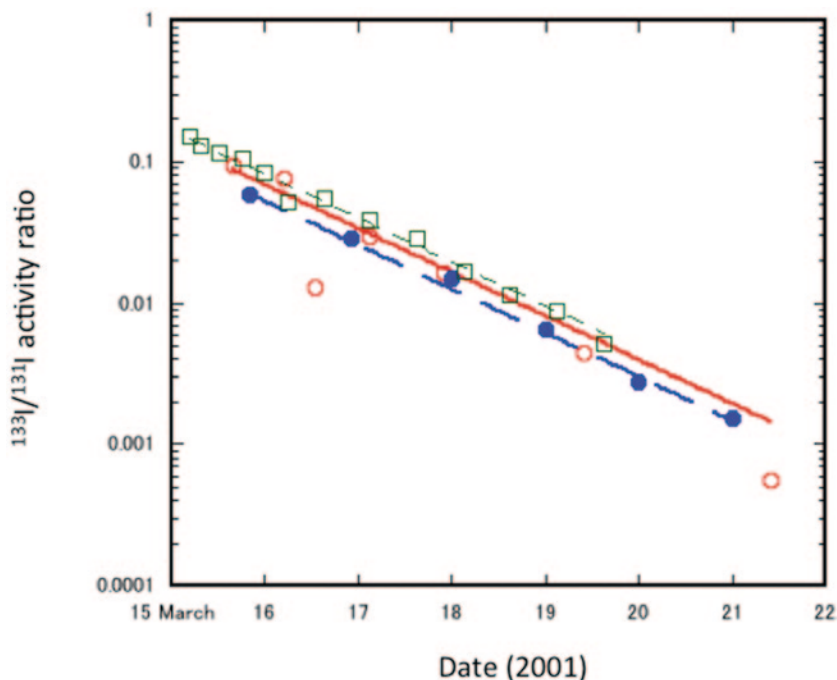


Fig. 6 Temporal variations of $^{133}\text{I}/^{131}\text{I}$ ratios in surface air observed at Tsukuba. *Open circle*: Tsukuba (Doi et al. 2013), *closed circle*: Inage (Amano et al. 2012), *open square*: Oarai (Furuta et al. 2011). The initial $^{133}\text{I}/^{131}\text{I}$ ratios on March 11 at Tsukuba, Inage, and Oarai were 1.5, 1.1, and 1.8, respectively

in Fig. 6. There was no geographical variation of temporal changes of the $^{133}\text{I}/^{131}\text{I}$ ratios observed at Tsukuba, Oarai, and Inage (Amano et al. 2012; Doi et al. 2013; Furuta et al. 2011; Kanai 2012), although lower $^{133}\text{I}/^{131}\text{I}$ ratios occurred at Tsukuba. A similar result has been obtained in US CTBTO network data (CTBTO, <http://www.ctbto.org/press-centre/highlights/2011/fukushima-related-measurements-by-the-ctbto/>), in which the temporal change of $^{133}\text{I}/^{131}\text{I}$ ratios measured in the US sites excellently correlated with the ORIGEN model (Biegalski et al. 2011). The temporal change of the $^{133}\text{I}/^{131}\text{I}$ ratio coincided with a decay curve of a decay constant ($\lambda_{133} - \lambda_{131}$). This suggests that the $^{133}\text{I}/^{131}\text{I}$ ratio at cease of nuclear fission in the reactors (March 11, 2011) was 1.4, which largely differed from that in estimated total release (0.26) as shown in Table 1 (RJG 2011).

The ^{134}Cs , ^{136}Cs (half-life: 13.16 d), and ^{137}Cs were detected in surface air at Oarai, Tsukuba, and Inage (Amano et al. 2012; Doi et al. 2013; Furuta et al. 2011; Kanai 2012). The temporal variation of the ^{137}Cs concentrations in surface air at Oarai and Tsukuba is shown in Fig. 7. The first peak of surface ^{137}Cs in the Kanto Plain occurred on March 15–16, 2011, which coincided with that of the total ^{131}I concentration and the ambient dose rate. On March 15, 2011, high radiocesium concentrations in surface air were observed at Oarai, Tsukuba, and Inage, where the

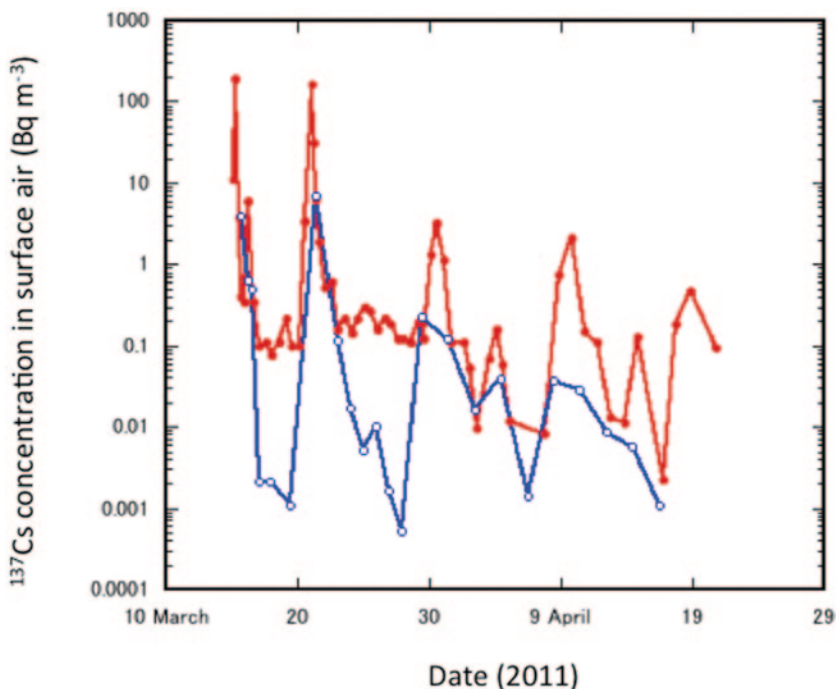


Fig. 7 Temporal variations of ^{137}Cs concentrations in surface air observed at Oarai and Tsukuba. This figure depicts the data from Doi et al. (2013) and Furuta et al. (2011)

^{137}Cs concentrations in surface air were $1.9 \times 10^2 \text{ Bq m}^{-3}$ (3 h mean value) (Furuta et al. 2011), 3.8 Bq m^{-3} (3 h mean value) (Doi et al. 2013), and 0.87 Bq m^{-3} (27 h mean value) (Amano et al. 2012), respectively. The ^{137}Cs concentrations in surface air at three sites decreased with increasing distance from the FDNPP, although a simple comparison between data cannot be carried out because of different air sampling time span. On March 18–20, the ^{137}Cs concentrations in surface air rapidly decreased to about three orders of magnitude lower than previous value in contrast of ^{131}I . The second peak of the surface ^{137}Cs in the Kanto Plain appeared on March 20–22, which corresponded to occurrence of the highest concentration (4.6 Bq m^{-3} (48 h mean value)) within the observation period. The observed maximum concentrations of ^{137}Cs in surface air at Oarai, Tsukuba, and Inage were 160 Bq m^{-3} (9 h mean value), 4.6 Bq m^{-3} (48 h mean value), and 6.1 Bq m^{-3} (26 h mean value), respectively. The ^{137}Cs concentration in surface air in the Kanto Plain, which showed some peaks in April–September, decreased, and ^{137}Cs can be still detected in air samples in early September, 2011 (detection limit: 0.05 mBq m^{-3}). It is noteworthy that radiocesium in surface air of Fukushima City has still been observed in the early 2012, whose concentrations were 0.1 to several mBq m^{-3} (MEXT 2012).

Isotope signature is an important tool to have better understanding of the environmental behaviors of the FDNPP-derived radionuclides. As it is well known that

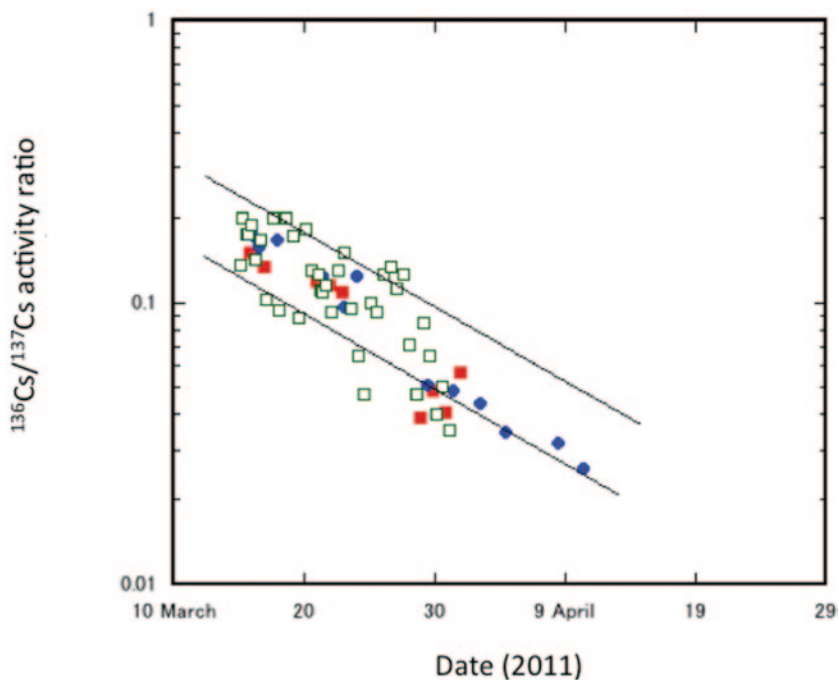


Fig. 8 Temporal variations of $^{136}\text{Cs}/^{137}\text{Cs}$ ratio in surface air. *Closed circle*: Tsukuba (Doi et al. 2013), *closed square*: Inage (Amano et al. 2012), *open square*: Oarai (Furuta et al. 2011). Solid lines show the radioactive decay curve of ^{136}Cs

^{134}Cs is not a direct fission product, ^{134}Cs is produced by neutron activation of ^{133}Cs , which is the decay product of ^{133}Xe present in nuclear reactors. $^{134}\text{Cs}/^{137}\text{Cs}$ ratios increase with burnup time of nuclear fuel. Mutual relationships between radiocesium in surface air were examined (Amano et al. 2012; Doi et al. 2013; Biegalski et al. 2011). The $^{134}\text{Cs}/^{137}\text{Cs}$ activity ratio in surface air at all sites including Japanese and the US stations, ranged from 0.9–1.2 as an average of 1.0 ± 0.1 , was fairly stable over the time of observation, which coincides with that of deposition (Amano et al. 2012; Hirose 2012). It must be noted that the $^{134}\text{Cs}/^{137}\text{Cs}$ activity ratio in the FDNPP-derived radionuclides is higher than that in the Chernobyl fallout ($^{134}\text{Cs}/^{137}\text{Cs}$ ratio: 0.5) (IAEA 1986; UNSCEAR 2000). Temporal change of the $^{136}\text{Cs}/^{137}\text{Cs}$ activity ratio is shown in Fig. 8. In contrast to the $^{134}\text{Cs}/^{137}\text{Cs}$ ratios, there was rather large variability of the $^{136}\text{Cs}/^{137}\text{Cs}$ ratio in surface air. The similar different nature of the $^{136}\text{Cs}/^{137}\text{Cs}$ ratio from the $^{134}\text{Cs}/^{137}\text{Cs}$ ratio was observed in the US monitoring sites (Biegalski et al. 2011). Although the $^{136}\text{Cs}/^{137}\text{Cs}$ ratio decreased exponentially, the $^{136}\text{Cs}/^{137}\text{Cs}$ ratios at three sites in Japan seemed to not fit in the simple decay curve of ^{136}Cs ; the $^{136}\text{Cs}/^{137}\text{Cs}$ ratios in late March–April 2011 were slightly lower than that in the period of the first and second peaks (March 15–22). The $^{136}\text{Cs}/^{137}\text{Cs}$ ratio was calculated to extrapolate at cease of reactors (March 11, 2011) from a decay curve of ^{136}Cs . The initial $^{136}\text{Cs}/^{137}\text{Cs}$ ratio ranged from 0.09 and 0.27. These findings

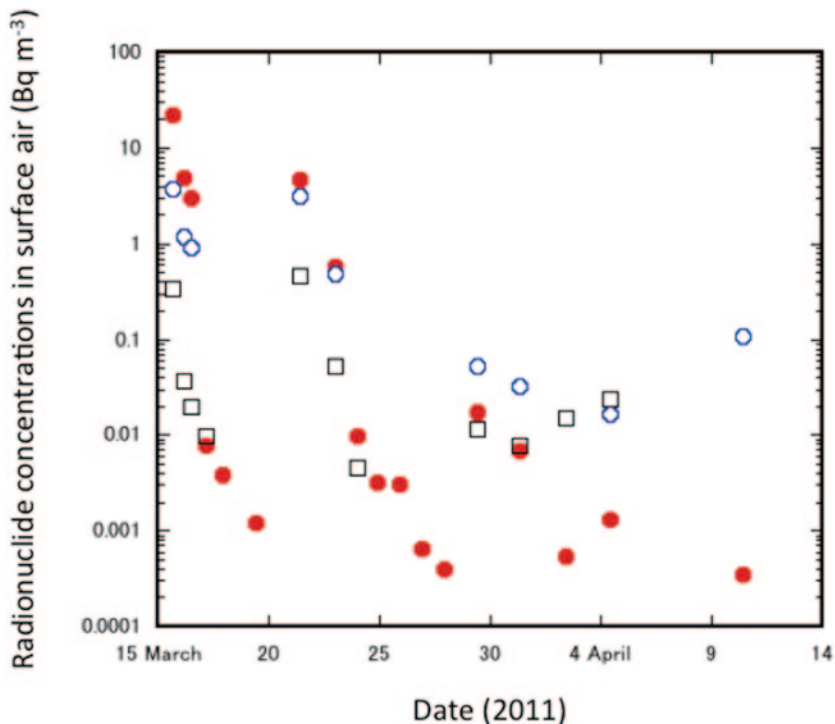


Fig. 9 Temporal variations of ^{132}Te (closed circle), $^{129\text{m}}\text{Te}$ (open circle), and $^{99\text{m}}\text{Tc}$ (open square) in surface air at Tsukuba. This figure depicts data from Doi et al. (2013)

suggest that there is no isotopic fractionation between ^{134}Cs and ^{137}Cs , whereas the $^{136}\text{Cs}/^{137}\text{Cs}$ ratio may change between major emission and following minor emission, although its cause is unknown. In this connection, Biegalski et al. (2012) mentioned that excess ^{137}Cs could be present in the samples due to the release of a damaged fuel in the Fukushima Daiichi spent nuclear fuel pools, taking into account the fact that temporal change of the $^{136}\text{Cs}/^{137}\text{Cs}$ ratios appear to be generally below the ORIGEN model (ORNL 2004). However, there is no report of the radioactivity release from the Fukushima Daiichi spent nuclear fuel pools. It is noteworthy that, determination of ^{136}Cs is rather complicated in the initial stage because of interference of short-lived radionuclides.

As other radionuclides, ^{132}Te (^{132}I), $^{129\text{m}}\text{Te}$ (^{129}Te), and ^{99}Mo ($^{99\text{m}}\text{Tc}$) were detected in the surface air samples at Tsukuba (Doi et al. 2013; Kanai 2012). Temporal variations of ^{132}Te , $^{129\text{m}}\text{Te}$, and ^{99}Mo ($^{99\text{m}}\text{Tc}$) in surface air at Tsukuba are shown in Fig. 9. ^{132}Te , $^{129\text{m}}\text{Te}$, and ^{99}Mo ($^{99\text{m}}\text{Tc}$) were detected on March 15, 2011, which coincided with the first detection of radioiodine and radiocesium. The maximum concentrations of ^{132}Te and $^{129\text{m}}\text{Te}$, which occurred on March 15, were 23 and 3.8 Bq m $^{-3}$, respectively, which corresponded to the maximum of radioiodine, whereas the

maximum ^{99}Mo ($^{99\text{m}}\text{Tc}$) concentration (0.46 Bq m^{-3}) occurred on March 20–22, corresponding to the maximum of radiocesium. The surface air concentrations of ^{132}Te , $^{129\text{m}}\text{Te}$, and ^{99}Mo ($^{99\text{m}}\text{Tc}$) exhibited three major peaks, which corresponded with that of ^{131}I and ^{137}Cs , and decreased to less than detection limit after mid-April 2011.

In order to elucidate difference of atmospheric behaviors between radionuclides, mutual relationships between ^{132}Te , $^{129\text{m}}\text{Te}$, and ^{99}Mo ($^{99\text{m}}\text{Tc}$) were examined, in which activity concentrations of short-lived radionuclides were corrected radioactive decay on March 11, 2011 (Doi et al. 2013). The decay-corrected ^{132}Te concentration in the surface air were correlated with that of the decay corrected $^{129\text{m}}\text{Te}$, in which the $^{129\text{m}}\text{Te}/^{132}\text{Te}$ ratio was 0.086 ± 0.005 . It is noteworthy that RJG (2011) documented the $^{129\text{m}}\text{Te}/^{132}\text{Te}$ ratio of 0.04 (Table 1). The ratios of the decay-corrected ^{132}Te , $^{129\text{m}}\text{Te}$, and $^{99\text{m}}\text{Tc}$ concentrations to the ^{137}Cs concentration in the surface air were calculated. The decay-corrected $^{132}\text{Te}/^{137}\text{Cs}$ and $^{129\text{m}}\text{Te}/^{137}\text{Cs}$ ratios were in the ranges of 4–65 and 0.3–5.4, respectively. Peaks of the decay-corrected $^{132}\text{Te}/^{137}\text{Cs}$ and $^{129\text{m}}\text{Te}/^{137}\text{Cs}$ ratios appeared on March 22–23 after occurrence of the maximum concentrations of ^{137}Cs on March 20–22. There was rather large variation of $^{132}\text{Te}/^{137}\text{Cs}$ and $^{129\text{m}}\text{Te}/^{137}\text{Cs}$ ratios, suggesting that atmospheric behaviors of radiotellurium differed from that of radiocesium. The decay-corrected ^{99}Mo ($^{99\text{m}}\text{Tc}$)/ ^{137}Cs , ranging from 0.16–22, showed larger variation than that of the decay-corrected $^{132}\text{Te}/^{137}\text{Cs}$ and $^{129\text{m}}\text{Te}/^{137}\text{Cs}$. The decay-corrected ^{99}Mo ($^{99\text{m}}\text{Tc}$)/ ^{137}Cs increased with time. These findings suggest that the atmospheric behavior of ^{99}Mo ($^{99\text{m}}\text{Tc}$) was significantly different from that of ^{137}Cs and ^{132}Te .

Atmospheric behaviors of the FDNPP-derived radionuclides depend on physical and chemical properties of radionuclide-bearing particles. Particle size distributions of the FDNPP-derived radionuclide-bearing particles collected at Tsukuba were determined during the periods of April 4–11 and April 14–21, 2011 (Doi et al. 2013) and April 29–May 12 and May 12–26, 2011 (Kaneyasu et al. 2012). The activity median aerodynamic diameters (AMAD) of ^{131}I bearing particles were calculated to be 0.7 and 0.7 μm in April 4–11, 2011 and in April 14–21, 2011, respectively, whereas the AMADs of ^{134}Cs and ^{137}Cs bearing particles were 1.8 and 1.5 μm in April 4–11, 2011, and 1.0 and 1.0 μm in April 14–21, 2011, respectively. In May, measurements of particle size distributions of radiocesium bearing particles (Kaneyasu et al. 2012) revealed that ^{137}Cs attached on sub-micrometer particles as did ^{134}Cs , are typically sulfate particles. These findings suggest that the particle size of the ^{131}I bearing particles differed from those of radiocesium, which implies that the dispersion and deposition behaviors of ^{131}I differed from that of ^{134}Cs and ^{137}Cs and that the particle size of the radio-caesium bearing particles changed with time. The result reveals that the FDNPP-derived ^{134}Cs and ^{137}Cs bearing particles observed in April 2011 were larger than that of the Chernobyl ^{137}Cs , which existed as sub-micrometer particles observed in Japan (Aoyama et al. 1992). These findings suggest that the FDNPP-derived radiocesium observed in April was preferentially removed from atmosphere by dry and wet deposition processes, and that, as a result, the FDNPP-derived radiocesium observed in May, existing as sub-micrometer particles, remained in the atmosphere (Kaneyasu et al. 2012). Paatero et al. (2012) estimated that a significant part of the FDNPP-derived radioactivity

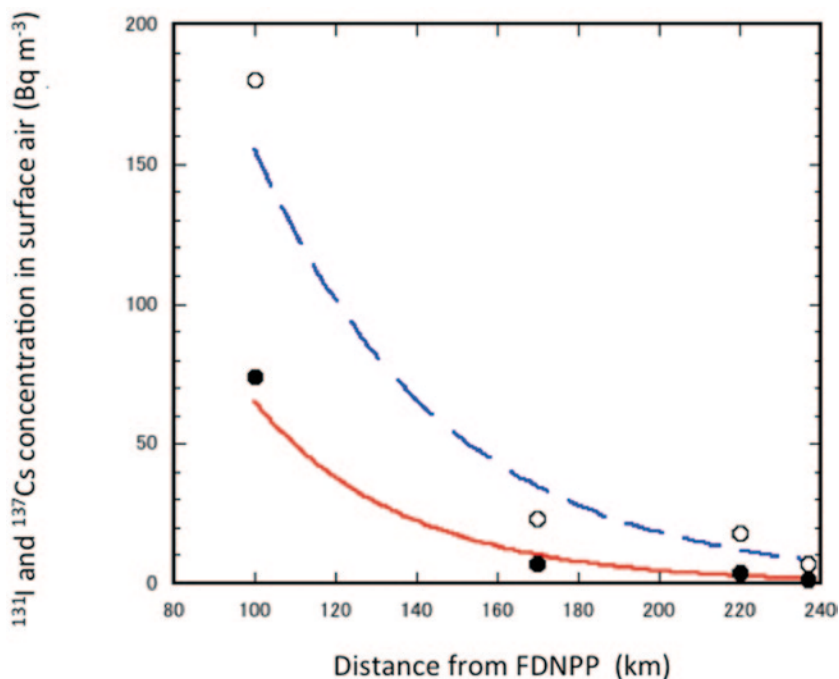


Fig. 10 Relationship between ^{131}I and ^{137}Cs surface air concentrations and distance from FDNPP. The 48 h mean values of ^{131}I and ^{137}Cs surface air concentrations during the period of March 20–21 were used. *Open circle*: ^{131}I , *closed circle*: ^{137}Cs . Used data were Oarai (Furuta et al. 2011), Tsukuba (Doi et al. 2013), Inage (Amano et al. 2012) and Setagaya (Tokyo: 237 km from the FDNPP <http://www.sangyo-rodo.metro.tokyo.jp/whats-new/measurement.html>)

is in hot particles from autoradiogram of a filter sample from 1–4 April 2011 at Mt. Zeppelin, Ny-Ålesund, Svalbard. It must be noted that there is no information about particle size of radionuclide-bearing particles in major radioactive plume occurring in the late March.

The surface air concentrations of the FDNPP-derived radionuclide decreased with distance from the FDNPP. The model simulation (Morino et al. 2011) revealed that the radioactive plume originating from the FDNPP flowed southwestward, in March 20–21, according to northeast wind. In order to elucidate the difference of the atmospheric behavior between ^{131}I and ^{137}Cs , the surface air concentrations of ^{131}I and ^{137}Cs at four sites corresponding to downstream of the FDNPP were potted as a function of distance from the FDNPP as shown in Fig. 10. The result reveals that the surface air concentrations of ^{131}I and ^{137}Cs decreased exponentially with distance shown in Fig. 10. The Apparent Half Decrease Distances (AHDD) of ^{131}I and ^{137}Cs can be calculated to be 32 and 26 km from the fitting curves, respectively. The AHDD of ^{131}I is longer than that of ^{137}Cs , which implies that ^{137}Cs emitted from the FDNPP is easily removed from atmosphere comparing with ^{131}I .

3.2 Global Monitoring

The Comprehensive Nuclear-Test-Ban Treaty (CTBT) (CTBTO, <http://www.ctbto.org/press-centre/highlights/2011/fukushima-related-measurements-by-the-ctbto/>) was adopted by the United Nations General Assembly on September 10, 1996 (CTBTO 2011). Within the CTBT, the International Monitoring System (IMS) was defined to monitor the world for nuclear explosions. The IMS comprises of four primary monitoring technologies: radionuclide, seismic, hydroacoustic, and infrasound. The FDNPP-derived radionuclides were first determined by global CTBTO network (CTBTO, <http://www.ctbto.org/press-centre/highlights/2011/fukushima-related-measurements-by-the-ctbto/>). The FDNPP-derived radionuclides were transported in the northern hemisphere in late March and April 2011; ^{131}I and ^{137}Cs were detected in the Asia (Bolsunovsky and Dementyev 2011; Kim et al. 2012), North America (Bowyer et al. 2011; Zhang et al. 2011), Europe (Lozano et al. 2011; Pittauerová et al. 2011), and Arctic (Paatero et al. 2012). The FDNPP-derived radionuclides had been detected around the northern Hemisphere in about two weeks and also in the southern Hemisphere about one month later.

In North America, on March 16, the FDNPP-derived gaseous radionuclides (^{133}Xe , $^{133\text{m}}\text{Xe}$, $^{131\text{m}}\text{Xe}$) were first detected by the Pacific Northwest Laboratory ($46^{\circ} 16'47''\text{N}$, $119^{\circ} 16'53''\text{W}$), located more than 7,000 km from the FDNPP (Bowyer et al. 2011). The maximum ^{133}Xe concentration (41 Bq m^{-3}) occurred on March 20. The second-highest values of radioactive xenon were observed on March 25. The radioactive cloud containing the FDNPP-derived radionuclides had crossed the Pacific Ocean and reached Canada (Sidney: 49.3°N , 123.2°W) on March 17, 6 days after the first emission from the accidental reactor (Zhang et al. 2011). In surface air, several volatile radionuclides, such as ^{131}I , ^{132}I , ^{132}Te , ^{134}Cs , ^{136}Cs , and ^{137}Cs , have been detected. On March 19, the surface air concentrations of ^{131}I , ^{132}I , and ^{132}Te reached their maximum values. Then on March 24, 5 days later the second-highest values of ^{131}I , ^{132}I , and ^{132}Te were observed as did maximum concentrations of ^{134}Cs , ^{136}Cs , and ^{137}Cs , which implies that the second high radioactive plume had reached Sidney BC. The temporal waves of radioiodine and radiocesium were larger than radioactive xenon.

In Europe, first the FDNPP-derived radionuclides were observed by the CTBTO station in Reykjavik, Iceland, on 20 March 2011 (CTBTO, <http://www.ctbto.org/press-centre/highlights/2011/fukushima-related-measurements-by-the-ctbto/>). From late March to early May, many air monitoring stations across Europe including the Arctic have documented traces of the FDNPP-derived radionuclides above the usual background levels, which were supported by resuspension of deposited radionuclides from the atmospheric nuclear testing and the Chernobyl accident for ^{137}Cs and emissions from radiotherapeutic facilities for ^{131}I . The elevated levels of radionuclides derived from the Fukushima NPP were detected at the surface air sampling stations in Portugal (Carvalho et al. 2012), Spain (Lozano et al. 2011), England (Beresford et al. 2012), Monaco (Pham et al. 2012), Italy (Clemenza et al. 2012), Germany (Pittauerová et al. 2011), Greece (Manolopoulou et al. 2011), and

Lithuania (Lujaniené et al. 2012). In Arctic, particle-bound ^{131}I was first detected at Mt. Zeppelin ($78^\circ 58'\text{N}$, $11^\circ 53'\text{E}$) from a sample collected between 25 March 2011 10:11 UTC and 28 March 2011 13:04 UTC (Paatero et al. 2012). The detected radionuclides were ^{133}Xe , ^{131}I , ^{134}Cs , ^{136}Cs , ^{137}Cs , and ^{132}Te . The model simulations (Takemura et al. 2011; Manolopoulou et al. 2011) revealed complicated long-range air mass transport from the FDNPP (Japan) across the North Pacific, the North America, and the North Atlantic Ocean to Europe. The most comprehensive radionuclide data over the Europe has been compiled by Masson et al. (2011). Trajectory analysis and comparison with ^7Be , which is a cosmogenic radionuclide produced in the upper troposphere and stratosphere, suggest that the FDNPP-derived radionuclides observed in the Europe were transported via upper troposphere (Lujaniené et al. 2012).

In Asia, the elevated levels of radionuclides derived from the FDNPP were detected at the surface air sampling stations in South Korea (Kim et al. 2012), Taiwan (Huh et al. 2012), and Vietnam (Long et al. 2012). For radioactivity monitoring stations in the Asia, the FDNPP-derived radionuclides (^{131}I , ^{134}Cs , and ^{137}Cs) were initially detected in the surface air on March 27–30. The highest concentrations of ^{131}I , ^{134}Cs , and ^{137}Cs appeared in April 6–7. The model simulation (Huh et al. 2012) revealed that the FDNPP-derived radioactive plume was predominantly transported toward the southwest under phases of northern-easterly winds in April 6–7. As a result, the highest radionuclide concentrations occurred in the southwest Japan (Kyushu) (Momoshima et al. 2012), the southern region of Korea, Taiwan, and Vietnam.

4 Radioactivity Deposition

4.1 Daily Deposition at Local and Regional Stations

Measurements of radionuclides in daily deposition samples, which include wet and dry depositions, started on March 18 at the Japanese Government monitoring stations (MEXT 2012). Daily radioactive deposition rates in 44 stations in Japan were recorded until the end of 2011. High radioactive deposition derived from the FDNPP accident occurred in wide area of the Kanto Plain and South Tohoku area from March 21–23, 2011. On the other hand, in the area adjacent to the FDNPP, high radioactive deposition occurred on March 15–16, although there was no daily radioactivity deposition record during the period of March 2011.

The temporal changes of the daily ^{131}I and ^{137}Cs deposition rates during the period of March to April are shown in Fig. 11a, b. Earliest daily deposition sampling in the Kanto Plain was carried out in Japan Chemical Analysis Center (Inage, Chiba Prefecture) (Amano et al. 2012). The first deposition of the FDNPP-derived radionuclides appeared on March 15, which coincided with the first arrival of the radioactive plume. The first peaks of ^{131}I and ^{137}Cs depositions, which were 2,400

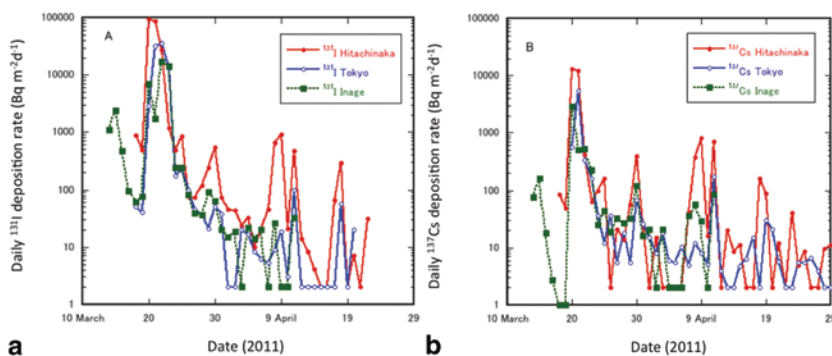


Fig. 11 Temporal changes of daily ^{131}I (a) and ^{137}Cs (b) deposition observed in the Kanto Plain. This figure depicts data from MEXT (2012). The value described as ND (not detected) is tentatively shown at 2 Bq m^{-2} in this figure

and $76 \text{ Bq m}^{-2}\text{d}^{-1}$, respectively, were observed at Inage on March 16. It must be noted that at the emergency stage of the accident, Government Monitoring documented only ^{131}I and ^{137}Cs as dominant radionuclides in deposition samples from the FDNPP accident by MEXT (2012). On March 20, the level of ^{131}I , a dominant radionuclide, at Hitachinaka (36.40°N , 140.54°E), which is located about 120 km south of the FDNPP, was $91 \text{ kBq m}^{-2}\text{d}^{-1}$ as a maximum value, and ^{137}Cs deposition at Hitachinaka was $13 \text{ kBq m}^{-2}\text{d}^{-1}$. High radionuclide deposition rates (^{131}I : $58 \text{ kBq m}^{-2}\text{d}^{-1}$, ^{137}Cs : $4.3 \text{ kBq m}^{-2}\text{d}^{-1}$) were observed at Yamagata (38.25°N , 140.33°E), which is about 110 km northwest of the FDNPP. On March 21, high deposition rates were observed in all of the monitoring stations of the Kanto Plain. In Inage, the highest daily deposition rates of ^{131}I and ^{137}Cs were measured on March 23 (^{131}I : $17 \text{ kBq m}^{-2}\text{d}^{-1}$, ^{137}Cs : $2.9 \text{ kBq m}^{-2}\text{d}^{-1}$) (Amano et al. 2012). The high radioactive deposition rates accompanied with rainfall continued until March 23. On March 24, the radioactive deposition rates decreased dramatically due to fine weather with coverage of high-pressure system. Most of the FDNPP-derived radionuclides, which were transported from the FDNPP by northeast wind, were deposited on land surface by rainfall during March 20–23. In April 2011, the monitoring stations in most of the Japan main islands had observed the FDNPP-derived radionuclides in the daily radioactive deposition samples. On May 2011, however, the daily deposition rate of the FDNPP-derived radionuclides in most of the Japanese monitoring stations decreased below detection limit except Fukushima City (37.75°N , 140.47°E), which is located about 60 km northwest of the FDNPP. In Fukushima City, in which radioactivity measurement in daily deposition samples started on April 1, 2011, ^{137}Cs was still detected in the daily deposition samples in the end of 2011 (Fig. 12).

The $^{131}\text{I}/^{137}\text{Cs}$ activity ratio in the daily deposition samples, ranged from 0.3–230, varied temporally and spatially. The $^{131}\text{I}/^{137}\text{Cs}$ activity ratio in total atmospheric release was estimated to be 11 (NSC 2011). Compared with the $^{131}\text{I}/^{137}\text{Cs}$ activity ratio at the initial release of radionuclides from the FDNPP, radioactive decay of ^{131}I was

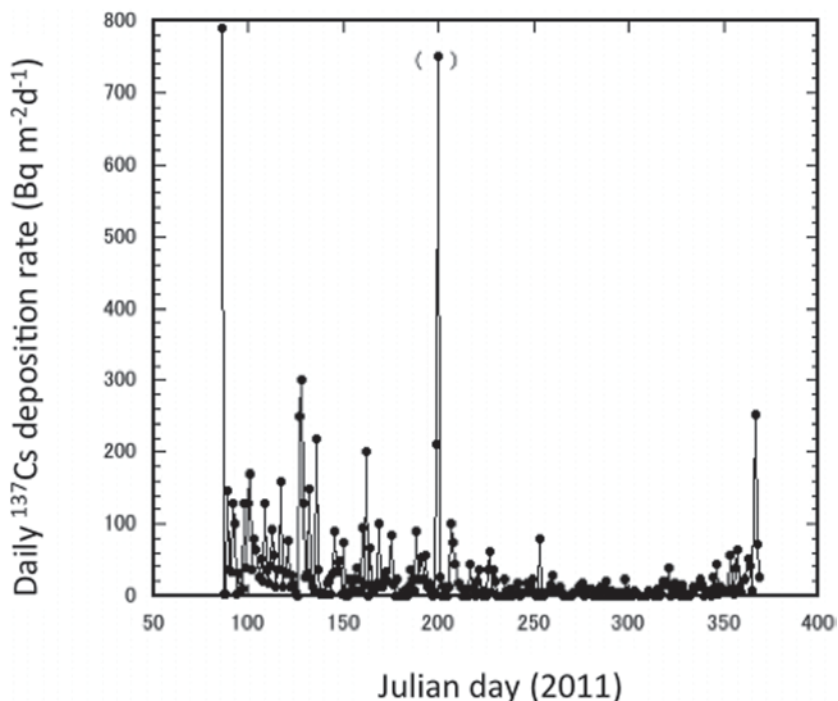


Fig. 12 Temporal changes of daily ^{137}Cs deposition observed at Fukushima City. This figure depicts data from MEXT (2012). The high value in July 2011 (shown with a parenthesis) contained large uncertainty due to measurement problems

corrected on March 11 when shutdown of nuclear reactors was conducted. The decay-corrected $^{131}\text{I}/^{137}\text{Cs}$ activity ratios ranged from 3.5–550, with a median value of 15. High decay-corrected $^{131}\text{I}/^{137}\text{Cs}$ activity ratios occurred on March 22–23, which corresponded to time just after occurrence of maximum deposition rates (March 20–21). Higher $^{131}\text{I}/^{137}\text{Cs}$ activity ratios appeared at the inland site (Utsunomiya: 36.60°N , 139.94°E), which means that the depositional behavior between ^{131}I and ^{137}Cs largely differed from each other. The $^{134}\text{Cs}/^{137}\text{Cs}$ activity ratios in the daily deposition samples were 1.0 (Amano et al. 2012).

4.2 Monthly Deposition at Local and Regional Stations

The Monitoring Centers in Local Governments have determined the FDNPP-derived radionuclides in monthly deposition samples. Iodine – ^{131}I , ^{134}Cs , and ^{137}Cs were measured as dominant radionuclides in the monthly deposition samples in all monitoring stations of Japan, whereas $^{129\text{m}}\text{Te}$, ^{129}Te , ^{136}Cs , $^{110\text{m}}\text{Ag}$, ^{95}Zr , ^{95}Nb (half-life: 35 d), ^{140}Ba , and ^{140}La (half-life: 1.68 days) were detected as minor radionu-

clides in the monthly deposition samples at the monitoring stations within 300 km of the FDNPP. For the monthly deposition, long-lived radionuclides (^{134}Cs , ^{137}Cs , and $^{110\text{m}}\text{Ag}$) are meaningful because the monthly deposition rates of the short-lived radionuclides are not well defined. Activity ratios of $^{134}\text{Cs}/^{137}\text{Cs}$ observed on March, ranged 1.0–1.1 as an average of 1.03, were constant in case when the monthly ^{137}Cs deposition was exceeded 100 Bq m^{-2} . The $^{134}\text{Cs}/^{137}\text{Cs}$ activity ratios on April and May at MEXT sites were from 0.99–1.09 with an average of 1.03 and from 0.93 to 1.04 with an average of 0.99, respectively (Hirose 2011). The result suggests that there were no spatial and temporal variations of the $^{134}\text{Cs}/^{137}\text{Cs}$ activity ratios in the monthly deposition samples during the period from March to May 2011. Activity ratios of $^{110\text{m}}\text{Ag}/^{137}\text{Cs}$ observed on March ranged 0.0009–0.006 as an average of 0.0019 (Hirose 2011).

The spatial distributions of the monthly ^{137}Cs deposition in March, April, and May are depicted in Fig. 13a, b, and c, respectively. The highest monthly ^{137}Cs deposition ($3,340 \text{ kBq m}^{-2}$) was observed in March at Futaba (Fukushima Prefecture) about 5 km of the FDNPP. The monthly ^{137}Cs depositions at the stations within 300 km of the FDNPP except Kofu (35.65°N , 138.57°E ; inland site) and the Japan Sea side sites (Niigata: 37.91°N , 139.04°E and Akita: 39.72°N , 140.10°E) were in the range from 1.1 kBq m^{-2} to 17 kBq m^{-2} , which are greater than the maximum monthly ^{137}Cs deposition (0.55 kBq m^{-2}) derived from the 1961–62 large-scale atmospheric nuclear testing observed at Koenji (Tokyo) in 1963 (Hirose et al. 2008; Igarashi et al. 2005). The results reveal that the high ^{137}Cs -deposited areas, comparable to the cumulative amount of the ^{137}Cs deposition at Tokyo until mid-1960 (about 7 kBq m^{-2}), appeared within a regional band from 100 to 300 km of the FDNPP. The spatial distribution of the monthly ^{137}Cs deposition on March 2011 revealed that the major deposition of the FDNPP-derived radionuclides occurred in the North Pacific coast and inland area of the east Honshu Island, whereas there was less contribution of the FDNPP-derived radionuclides in the Japan Sea side sites of the east Honshu Island. These findings suggest that the transport of the radioactive plume is strongly affected by land topography, and that most of the FDNPP-derived radionuclides might be injected in the boundary layer (about 1,000 m). Model simulation (Morino et al. 2011) revealed that land topography controls the transport of the FDNPP-derived radioactive plume.

The higher monthly ^{137}Cs deposition (0.17 Bq m^{-2}), which was one order of magnitude higher than pre-Fukushima levels (Igarashi et al. 2005), was observed on March at Fukuoka (33.51°N , 130.50°E) and Uruma (26.31°N , 127.90°E , Okinawa), which are located about 1,050 and 1,750 km southwest of the FDNPP, respectively. Detection of ^{131}I and ^{134}Cs in the same sample revealed that the FDNPP-derived radionuclides were transported to Fukuoka and Uruma in late March. The highest monthly deposition rates of radiocesium occurred at Fukuoka and Uruma in April 2011; the monthly ^{137}Cs depositions at Fukuoka and Uruma were 0.5 and 3.7 Bq m^{-2} . It must be noted that the ^{137}Cs deposition at Uruma is higher than that at Fukuoka. Model simulation (Takemura et al. 2011) suggested that the FDNPP-derived radioactivity plume spread far eastern Siberia on March 24. Another model simulation (Masson et al. 2011) revealed that the FDNPP-derived radioactive plume

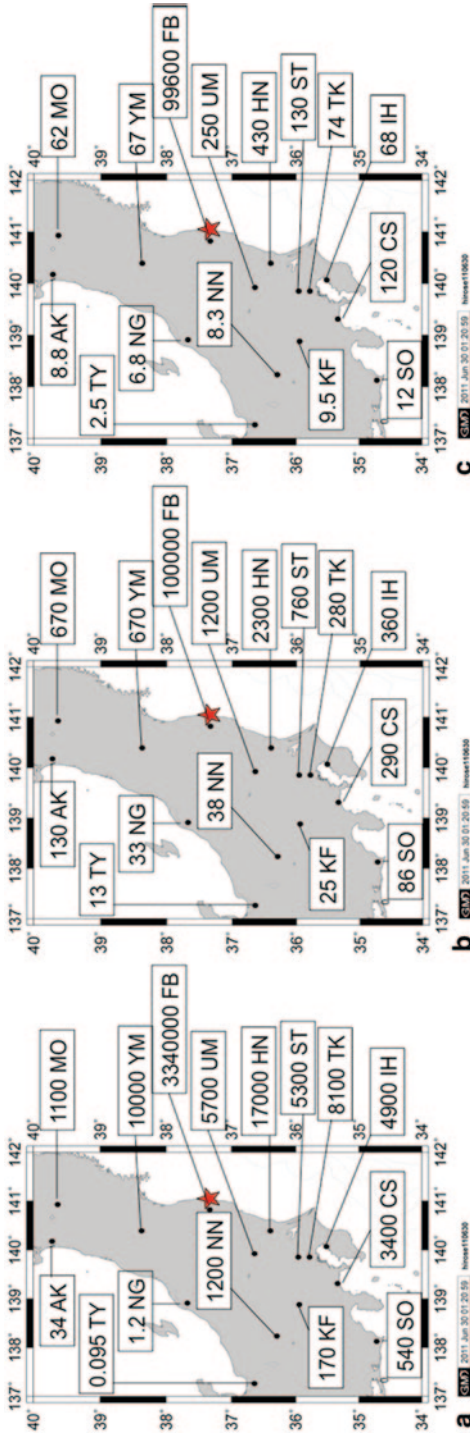


Fig. 13 Spatial distributions of monthly ^{137}Cs deposition observed in Japan. (Unit: Bq m^{-2}) **a** March, **b** April, **c** May. *AK* Akita, *MO* Morioka, *YM* Yamagata, *FB* Futaba, *NG* Niigata, *UM* Utsunomiya, *HN* Hitachinaka, *ST* Saitama, *TK* Tokyo, *IH* Ichihara, *CS* Chigasaki, *SO* Shizuoka, *KF* Kofu, *NN* Nagano, *TY* Toyama. Data were cited from MEXT (2012)

was predominantly transported toward the southwest under phases of northern-easterly winds on April 6–7. It is likely that, the FDNPP-derived radionuclides observed at Fukuoka and Uruma were transported via the east Siberia or the North Pacific southwest of Honshu Islands rather than round the globe.

On April, higher monthly ^{137}Cs depositions were observed at the North Pacific side stations and East Japan inland stations, although the levels decreased markedly. This suggests that the atmospheric emission of radionuclides from the FDNPP continued on April 2011, although the release rate decreased dramatically. On the other hand, the monthly ^{137}Cs deposition increased at southwest sites in Japan and at the Japan Sea side sites comparing with that on March, suggesting that the FDNPP-derived radioactive cloud dominantly affected north part of the Northern Hemisphere atmosphere. On May, the monthly ^{137}Cs depositions decreased at all of the monitoring stations of Japan (Fig. 13c), although higher ^{137}Cs depositions were observed within 300 km of the FDNPP. On August, the monthly ^{137}Cs depositions at most of the monitoring stations in southwest Japan decreased below detection limit.

4.3 Atmospheric Half-Life of FDNPP-Derived ^{137}Cs

In order to elucidate depositional behaviors of the FDNPP-derived radionuclides, it is important to examine the temporal change of the monthly ^{137}Cs deposition. The monthly ^{137}Cs deposition at the sites in 300 km of the FDNPP except Futaba exhibited exponential decrease during the period of March to June as shown in Fig. 14. Apparent half-lives of the FDNPP-derived atmospheric ^{137}Cs ranged from 8.8 days for Tokyo to 14 days for Morioka (39.70°N, 141.16°E) (Hirose 2011). The apparent atmospheric half-life of the FDNPP-derived ^{137}Cs is similar to the residence time (8 days) estimated for ^{210}Pb over the west central United States, based on radioactive equilibrium of ^{210}Pb with its short-lived progenies (Moore et al. 1973). Lambert et al. (1982) estimated a global mean aerosol residence time of 6.5 days by using atmospheric inventories of ^{222}Rn and ^{210}Pb extrapolated from the observations and computing the ^{210}Pb deposition sink to balance ^{222}Rn decay. The residence time of tropospheric aerosols inferred from a global three-dimensional simulation of ^{210}Pb was 5–10 days, which depends on season and latitude (Balkanski et al. 1993). On the other hand, longer troposphere residence time of aerosols (about 30 days) was obtained from radioactive debris of atmospheric nuclear explosions (Katsuragi 1983). A similar long residence time was estimated for the Chernobyl ^{137}Cs (25 days) (Aoyama 1988), which was emitted as sub-micrometer particles (Hirose 1995). The residence times of aerosols in troposphere, which are in the range of 5–30 days, have been determined by natural and anthropogenic radionuclides, which depend on particles size and altitude (Ehhalt 1973). The shorter half-life of the FDNPP-derived ^{137}Cs suggests that most of the FDNPP-derived radionuclides were injected into the lower layer of the troposphere and/or emitted as larger particles in the atmosphere. As another possible process, the apparent half-life of the FDNPP-derived ^{137}Cs may partly reflect a history of the atmospheric

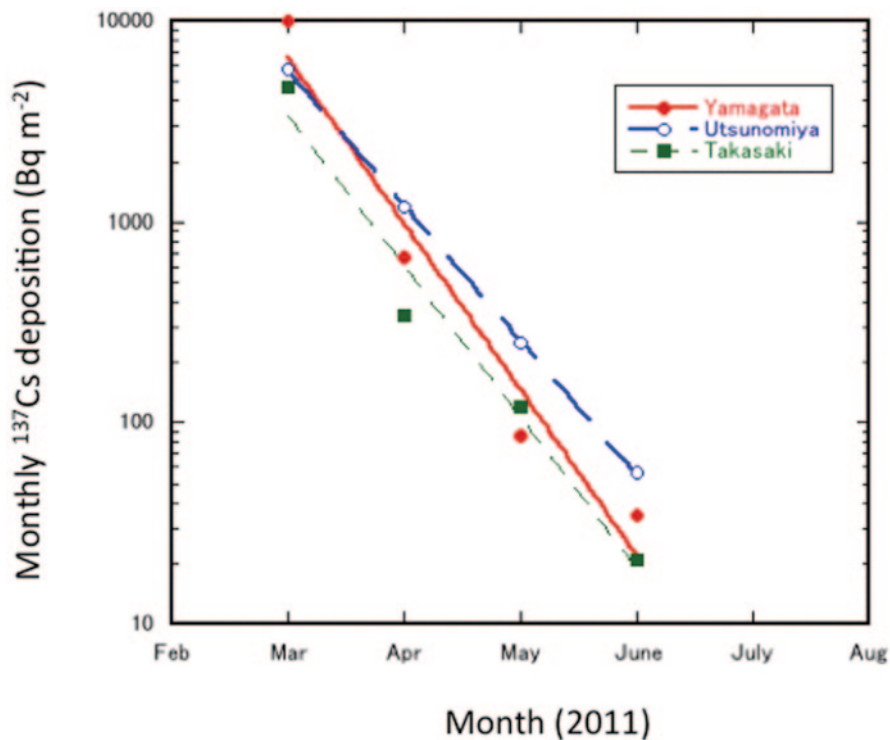


Fig. 14 Temporal changes of monthly ^{137}Cs deposition observed at several sites of east Honshu Island. Data were cited from MEXT (2012). The apparent half-lives of atmospheric ^{137}Cs at Yamagata, Utsunomiya, and Takasaki were 11, 13.5, and 12 days, respectively

emission because, the radioactive emission from the FDNPP continued as of the end of 2011, although the emission rate of radioactivity dramatically decreased (TEPCO 2011). In Futaba, the monthly ^{137}Cs deposition showed different history from other monitoring stations as shown in Fig. 15; rapid decrease of the monthly ^{137}Cs deposition occurred from March to April, after that, the decrease rate of the monthly ^{137}Cs deposition was slower than that of other stations in the corresponding period. It is likely that, the monthly ^{137}Cs deposition at Futaba was strongly affected by the atmospheric emission from the FDNPP.

The monthly ^{137}Cs deposition after July, 2011 at the monitoring stations in the Kanto Plain exhibited slower decrease rates as shown in Fig. 15, although ^{137}Cs cannot be detected in the monthly deposition samples for most of the monitoring stations in the south western region of Japan. Most of the monitoring stations in the Kanto Plain have reported meaningful amounts of the monthly radiocesium deposition in the end of 2011 (MEXT 2012). The relatively high levels of the radiocesium deposition rates in summer—winter 2011 may be supported by re-suspension of radiocesium deposited on land surface (Hirose et al. 2012; Igarashi et al. 2003, 2009). Another possible source may be subsequent emission of radiocesium from the FDNPP.

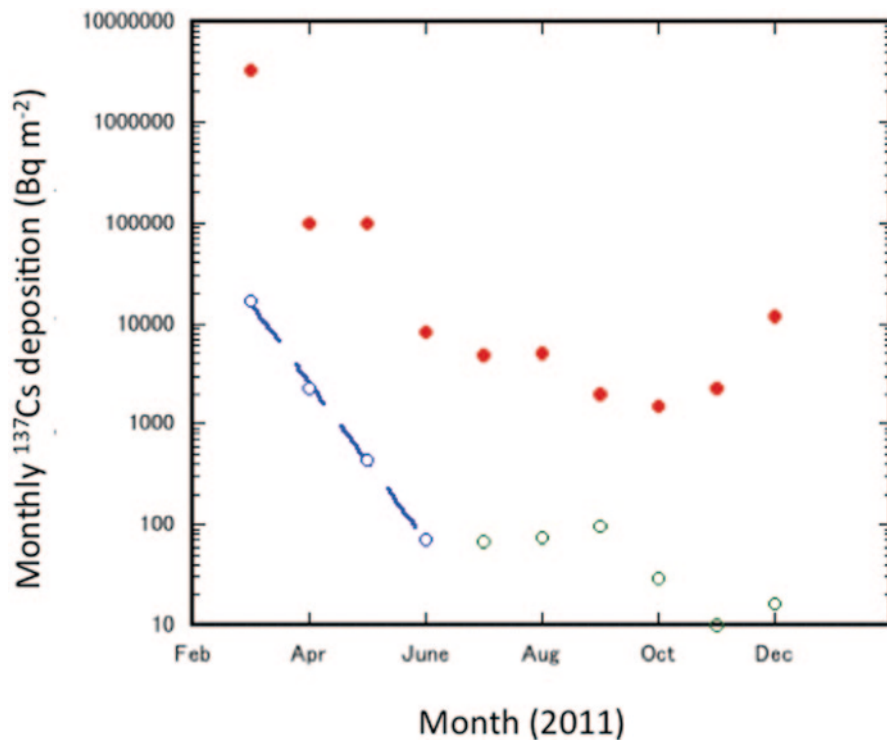


Fig. 15 Temporal changes of monthly ^{137}Cs deposition observed at sites near the FDNPP. *Closed circle*: Futaba, *open circle*: Hitachinaka. The apparent half-life of atmospheric ^{137}Cs at Hitachinaka in March–June was 11.5 days

4.4 Deposition Behavior of FDNPP-Derived Radionuclides

Deposition velocity is a useful tool to have better understanding of the atmospheric behavior of the FDNPP-derived radionuclide: deposition velocity V_d (m s^{-1}) = deposition flux ($\text{Bq m}^{-2}\text{s}^{-1}$)/surface air concentration (Bq m^{-3}). Amano et al. (2012) (Amano et al. 2012) have determined the deposition velocities of the FDNPP-derived ^{131}I and ^{137}Cs during the periods March 14–17 and March 21–24, corresponding to the first arrival (no rainfall) and the second arrival (heavier rainfall: 38 mm), respectively. The deposition velocities in the first arrival of the radioactive plume, corresponding to dry deposition velocity, were around 0.002 – 0.003 m s^{-1} for ^{134}Cs and ^{137}Cs and 0.001 – 0.003 m s^{-1} for ^{131}I . The dry deposition velocities of the Chernobyl fallout were determined to be 0.00035 – 0.0058 m s^{-1} for ^{134}Cs and ^{137}Cs and 0.00023 – 0.00095 m s^{-1} for ^{131}I (Aoyama et al. 1992). The dry deposition velocities of the FDNPP-derived radionuclides are of the same order of magnitude as those of the Chernobyl fallout, although the dry deposition velocities depend on size and chemical characteristics of radionuclide-bearing particles. The deposition velocities in the second arrival of the radioactive plume, corresponding to wet deposition velocity, were around 0.01 – 0.14 m s^{-1} for ^{134}Cs and ^{137}Cs and 0.004 – 0.03 m s^{-1}

for ^{131}I . The wet deposition velocities of the Chernobyl fallout were determined to be $0.0026\text{--}0.11\text{ m s}^{-1}$ for ^{137}Cs (Hirose et al. 1993). The wet deposition velocities of the FDNPP-derived radiocesium are of the same order of magnitude as those of the Chernobyl fallout. It is noteworthy that, the wet deposition velocities depend on size and chemical characteristics of radionuclide-bearing particles and meteorological conditions such as rainfall intensity (Hirose et al. 1993). The wet deposition velocities of the FDNPP-derived radionuclides were more than one order of magnitude greater than their dry deposition velocities, which implies that the FDNPP-derived radionuclides were deposited on land surface by wet deposition processes rather than dry deposition. Furthermore, these findings suggest that the FDNPP-derived radiocesium is slightly easily removed from the atmosphere by wet and dry deposition processes comparing with the FDNPP-derived radioiodine.

5 Mapping of Radioactivity Deposition

Serious radioactivity deposited area due to the FDNPP fallout spread about 300 km of the FDNPP, which suggested with deposition data (Hirose 2011) and model simulation (Morino et al. 2011). In order to effectively operate radiation protection to the FDNPP-derived radioactivity, it is essential to construct detail radioactivity contamination map of land surface. The mapping of radioactivity-contaminated area has been performed by radioactivity measurements based on high dense soil sampling in Fukushima Prefecture (Yoshida and Takahashi 2012) and airborne monitoring with NaI (TI) detectors and helicopter. The airborne monitoring of radiation has been conducted by MEXT with cooperation of the US DOE since April 6, 2011 (Lyons and Colton 2012). Comparison between airborne monitoring data and high dense soil data provides the most adequate conversion factors to estimate the FDNPP-derived radionuclide deposition from airborne gamma-ray measurement. The airborne monitoring can be realized in the radiocesium-contaminated area with deposition density of more than 10 kBq m^{-2} . The map of the FDNPP-derived ^{137}Cs deposition is shown in Fig. 16. The high radiocesium-contaminated area due to the Fukushima fallout spread narrow area northwestward of the FDNPP. Another typical feature is that higher contaminated areas are present in Fukushima Basin besides the northern and southern mountains, the mountainside of the north Kanto Plain, and the central part of the Kanto Plain. This finding suggests that the FDNPP fallout was strongly governed by land topography and geographical distribution of rainfall.

6 Conclusion

The radioactive plume was emitted from the FDNPP since March 12, 2011. Dominant radioactive emission in atmosphere occurred in March 15–16, 2011 (Chino et al. 2011). The FDNPP-derived radionuclides were detected in surface air of land

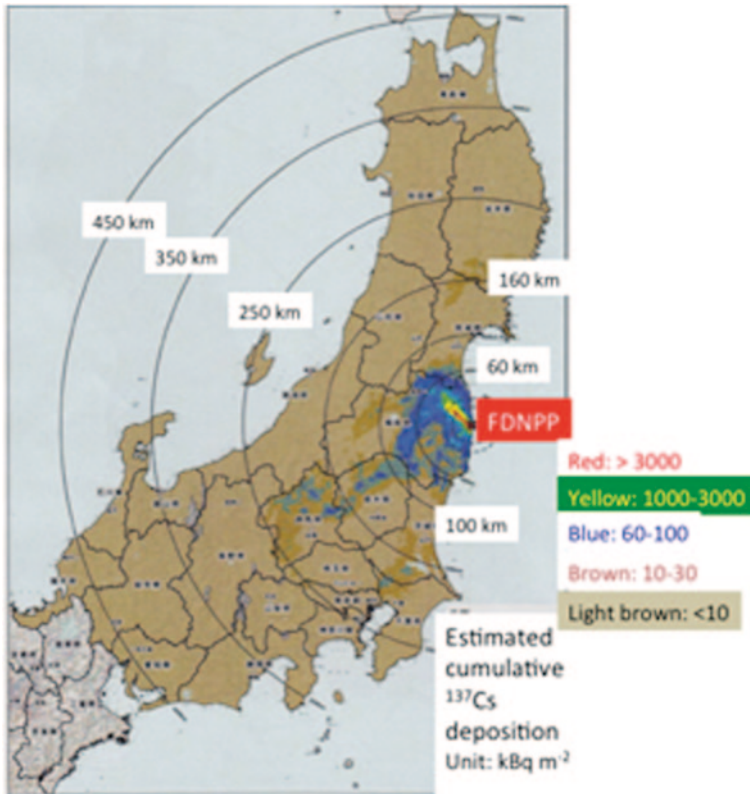


Fig. 16 Spatial distribution of FDNPP-derived ^{137}Cs deposition measured by airborne monitoring. This figure is depicted on basis of figure in MEXT (2012)

monitoring stations (especially in the Kanto Plain) since March 15, 2011, which was consistent with elevated ambient dose rate. The highest concentrations of the FDNPP-derived radionuclides in surface air at the monitoring stations of the Kanto Plain occurred in March 15–16 and March 20–22 as a result of transport of the radioactive plume from the FDNPP. Detected radionuclides were ^{133}I , ^{132}I , ^{131}I , ^{134}Cs , ^{136}Cs , ^{137}Cs , $^{129\text{m}}\text{Te}$ (^{129}Te), $^{99\text{m}}\text{Mo}$ ($^{99\text{m}}\text{Tc}$), $^{110\text{m}}\text{Ag}$, ^{95}Nb , and ^{140}Ba (^{140}La). In late March and April, global network of radioactivity monitoring in the northern hemisphere detected the FDNPP-derived radioactivity fallout. The surface air concentrations of the FDNPP-derived radionuclides decreased with distance from the FDNPP. When radioactive decay is corrected at cease of nuclear fission in the FDNPP, the ratios between isotopes are almost constant during the sampling period; the $^{133}\text{I}/^{131}\text{I}$, $^{134}\text{Cs}/^{137}\text{Cs}$, $^{136}\text{Cs}/^{137}\text{Cs}$, $^{129\text{m}}\text{Te}/^{132}\text{Te}$ ratios were 1.4, 1.0, 0.09–0.27, and 0.09, respectively. On the other hand, there were larger variations between elements; the decay-corrected $^{131}\text{I}/^{137}\text{Cs}$, $^{132}\text{Te}/^{137}\text{Cs}$, and $^{99\text{m}}\text{Tc}/^{137}\text{Cs}$ at Tsukuba were in the ranges of $8\text{--}1.0 \times 10^3$, 4 to 65, and 0.16 to 22, respectively. Large variations of the $^{131}\text{I}/^{137}\text{Cs}$, $^{132}\text{Te}/^{137}\text{Cs}$, and $^{99\text{m}}\text{Tc}/^{137}\text{Cs}$ ratios suggest that

atmospheric emission of the FDNPP-derived radionuclides and removal processes of these radionuclides in the atmosphere were affected largely by the chemical and physical properties of elements. In fact, significant amounts of ^{131}I and ^{133}I existed as gaseous form, whereas radiocesium in surface air on April attached relatively larger particles ($> 1 \mu\text{m}$).

As a result of snowfall and southwest wind on March 15–16, serious radioactive contaminated area appeared in Fukushima Prefecture (MEXT 2012). The Kanto plain was mainly contaminated by the FDNPP-derived radionuclides due to the movement of radioactive cloud by northeast wind and following rainfall during March 20 to 23. The airborne monitoring is an effective tool to realize the mapping of radioactivity-contaminated area. Recent model simulation can reproduce high radioactive deposition area and global dispersion of the FDNPP-derived radionuclides. The apparent residence time of the FDNPP-derived radionuclides observed in the Kanto plain and northeast Honshu Island is about 12 days, which suggests that major radioactive materials emitted from the FDNPP accident were injected into the lower layer of the troposphere.

The FDNPP accident is still ongoing at the end of 2011 (TEPCO 2011), although major atmospheric emission of radionuclides has been ceased in the end of March 2011 apparently. To have better understanding of the environmental behaviors of the FDNPP-derived radionuclides, including factors controlling variability of temporal change between radionuclides, it is necessary to know physical and chemical properties of the FDNPP-derived radionuclides in addition to detail time course of radioactivity emission at accidental reactors. Now, there is only limited information on the environmental impact of the FDNPP-derived radioactivity, although huge amounts of the environmental radioactivity data related to the FDNPP accident have been documented. In order to do adequate response to public concern, further investigation is required.

Acknowledgment Author thanks monitoring staffs and officers of MEXT for great efforts to measure environmental radioactivity.

References

- Amachi S, Kamagata Y, Kanagawa T, Muramatsu Y (2011) Bacteria mediate methylation of iodine in marine and terrestrial environment. *Appl Environ Microbiol* 67:2918–2722
- Amano H, Akiyama M, Chunlei B, Kawamura T, Kishimoto T, Kuroda T et al (2012) Radiation measurements in the Chiba Metropolitan area and radiological aspects of fallout from the Fukushima Daiichi Nuclear Power Plants accident. *J Environ Radioact* 111:42–52
- Aoyama M (1988) Evidence of stratospheric fallout of caesium isotopes from the chernobyl accident. *Geophys Res Lett* 15:327–330
- Aoyama M, Hirose K, Takatani S (1992) Particle size dependent dry deposition velocity of the Chernobyl radioactivity. In *Hemisphere Precipitation scavenging and atmospheric exchange processes*; Fifth International Conference, vol 3, pp 1581–1593
- Aoyama M, Tsumune D, Hamajima Y (2012) Budgets and temporal change of radiocesium distribution released from Fukushima NPP accidents in the North Pacific Ocean, 2012 Ocean Science Meeting, abstract ID10092

- Balkanski YJ, Jacob DJ, Gardner GM, Graustein WC, Turekian KK (1993) Transport and residence time of tropospheric aerosols inferred from a global three-dimensional simulation of ^{210}Pb . *J Geophys Res* 98:20573–20586
- Beresford NA, Barnett CL, Howard BJ, Howard DC, Wells C, Tyler AN, Bradley S, Copplestone D (2012) Observations of Fukushima fallout in Great Britain. *J Environ Radioact* 114:48–53. doi:10.1016/j.jenvrad.2011.12.008
- Biegalski SR, Bowyer TW, Eslinger PW, Friese JA, Greenwood LR, Haas DA, Hayes JC, Hoffman I, Keillor M, Miley HS, Moring M (2011) Analysis of data from sensitive U.S. monitoring stations for the Fukushima Dai-ichi nuclear reactor accident. *J Environ Radioact* 114:15–21
- Bolsunovsky A, Dementyev D (2011) Evidence of the radioactive fallout in the center of Asia (Russia) following the Fukushima Nuclear Accident. *J Environ Radioact* 102:1062–1064
- Bowyer TW, Biegalski SR, Cooper M, Eslinger PW, Haas D, Hayes JC et al (2011) Elevated radionuclides detected remotely following the Fukushima nuclear accident. *J Environ Radioact* 102:681–687
- Carvalho FP, Reis MC, Oliveira JM, Malta M, Silva L (2012) Radioactivity from Fukushima nuclear accident detected in Lisbon, Portugal. *J Environ Radioact* 114:152–156
- Chino M, Nakayama H, Nagai H, Terada H, Katata G, Yamazawa H (2011) Preliminary estimation of released amounts of ^{131}I and ^{137}Cs accidentally discharged from the Fukushima Daiichi nuclear power plant into the atmosphere. *J Nucl Sci Technol* 48:1129–1134
- Clemenza M, Fiorini E, Previtali E, Sala E (2012) Measurement of airborne ^{131}I , ^{134}Cs and ^{137}Cs due to the Fukushima reactor incident in Milan (Italy). *J Environ Radioact* 114:152–156
- CTBTO (Comprehensive Nuclear-Test-Ban Treaty Organization) (2011). <http://www.ctbto.org/press-centre/highlights/2011/fukushima-related-measurements-by-the-ctbto/>
- Doi T, Masumoto K, Toyoda A, Tanaka A, Shibata Y, Hirose K (2013) Anthropogenic radionuclides in the atmosphere observed at Tsukuba: Characteristics of the radionuclides derived from Fukushima. *J Environ Radioact* 122:55–62
- Ehhalt DH (1973) Turnover times of ^{137}Cs and HTO in the troposphere and removal rates of natural particles and vapor. *J Geophys Res* 78:7076–7086
- Furuta S, Sumiya S, Watanabe H, Nakano M, Imaizumi K, Takeyasu M et al (2011) (In Japanese) Results of the environmental radiation monitoring following the accident at the Fukushima Daiichi nuclear power plant—Interim report (ambient radiation dose rate, radioactivity concentration in the air and radioactivity concentration in the fallout). *JAEA-Review* 2011-035:1–84
- Hirose K (1995) Geochemical studies in the Chernobyl radioactivity in environmental samples. *J Radioanal Nucl Chem Articles* 197:331–342
- Hirose K (2012) 2011 Fukushima Daiichi nuclear power plant accident: summary of regional radioactivity deposition monitoring results. *J Environ Radioact* 111:13–17
- Hirose K, Takatani S, Aoyama M (1993) Wet deposition of long-lived radionuclides derived from the Chernobyl accident. *J Atmos Chem* 17:61–73
- Hirose K, Igarashi Y, Aoyama M (2008) Analysis of 50 years records of atmospheric deposition of long-lived radionuclides in Japan. *Appl Radiat Isot* 66:1675–1678
- Hirose K, Kikawada Y, Igarashi Y (2012) Temporal variation and provenance of thorium deposition observed at Tsukuba, Japan. *J Environ Radioact* 108:24–28
- Huh CA, Hsu S-C, Lin C-Y (2012) Fukushima-derived fission nuclides monitored around Taiwan: free tropospheric versus boundary layer transport. *Earth Planet Sci Lett* 319–320:9–14
- IAEA (1986) Summary report on the post-accident review meeting on the Chernobyl' accident. Safety Series No. 75-INSAG-1
- Igarashi Y, Aoyama M, Hirose K, Miyao T, Nemoto K, Tomita M, Fujikawa T (2003) Resuspension: decadal monitoring time series of the anthropogenic radioactivity deposition in Japan. *J Rad Res* 44:319–328
- Igarashi Y, Aoyama M, Hirose K, Povinec PP, Yabuki S (2005) What anthropogenic radionuclides (^{90}Sr and ^{137}Cs) in atmospheric deposition, surface soils and Aeolian dusts suggest for dust transport over Japan. *Water Air Soil Poll: Focus* 5:51–69

- Igarashi Y, Inomata Y, Aoyama M, Hirose K, Takahashi H, Shinoda Y, Sugimoto N, Shimizu A, Chiba M (2009) Possible change in Asian dust source suggested by atmospheric anthropogenic radionuclides during the 2000s. *Atmos Environ* 43:2971–2980
- IPG (Ibaraki Prefectural Government) (2011) http://www.pref.ibaraki.jp/earthquake/doserate_2011.html. Accessed Mar 2014
- Kanai Y (2012) Monitoring of aerosols in Tsukuba after Fukushima Nuclear Power Plant incident in 2011. *J Environ Radioact* 111:33–37
- Kaneyasu N, Ohashi H, Suzuki F, Okuda T, Ikemori F (2012) Sulfate aerosol as a potential transport medium of radiocesium from the Fukushima nuclear accident. *Environ Sci Technol* 46:5720–5726
- Katsuragi Y (1983) A study of ^{90}Sr fallout in Japan. *Pap Meteor Geophys* 33:277–291
- Kim C-K, Byun J-I, Chae J-S, Choi H-Y, Choi S-W, Kim D-J et al (2012) Radiological impact in Korea following the Fukushima nuclear accident. *J Environ Radioact* 111:70–82
- Lambert G, Polian G, Sanak J, Ardouin B, Buisson A, Jegou A, Lerouley JC (1982) Cycle du radon et de ses descendants: application à l'étude des échanges troposphère-stratosphère. *Ann Geophys* 38:497–531
- Long NQ, Truong Y, Hien PD, Binh NT, Sieu LN, Giap TV, Phan NT (2012) Atmospheric radionuclides from the Fukushima Dai-ichi nuclear reactor accident observed in Vietnam. *J Environ Radioact* 111:53–58
- Lozano RL, Hernández-Ceballos MA, Adame JA, Casas-Ruiz M, Sorribas M, San Miguel EG, Bolívar JP (2011) Radioactive impact of Fukushima accident on the Iberian Peninsula: evolution and plume previous pathway. *Environ Int* 37:1259–1264
- Lujanienė G, Bycenkienė S, Povinec PP, Gera M (2012) Radionuclides from the Fukushima accident in the air over Lithuania: measurement and modeling approaches. *J Environ Radioact* 114:71–80
- Lyons C, Colton D (2012) Aerial measuring system in Japan. *Health Phys* 102:509–515
- Manolopoulou M, Vagenas E, Syoulos S, Loannidou A, Papastefanou C (2011) Radioiodine and radiocesium in Thessaloniki, Greece due to the Fukushima nuclear accident. *J Environ Radioact* 102:796–797
- Masson O et al (2011) Tracking of airborne radionuclides from the damaged Fukushima Dai-ichi nuclear reactors by European networks. *Environ Sci Technol* 45:7670–7677
- MEXT (Ministry of Education, Culture, Sports, Science and Technology) (2012) <http://www.mext.go.jp/amenu/saigaijyouhou/syousai/1303856.htm>. Accessed Mar 2012
- Momoshima N, Sugihara S, Ichikawa R, Yokoyama H (2012) Atmospheric radionuclides transported to Fukuoka, Japan remote from the Fukushima Daiichi nuclear power complex following the nuclear accident. *J Environ Radioact* 111:28–32
- Moore HE, Poet SE, Martell EA (1973) ^{222}Rn , ^{210}Pb , ^{210}Bi , and ^{210}Po profiles and aerosol residence times versus altitude. *J Geophys Res* 78:7065–7075
- Morino Y, Ohara T, Nishizawa M (2011) Atmospheric behavior, deposition, and budget of radioactive materials from the Fukushima Daiichi nuclear power plant in March 2011. *Geophys Res Lett* L00G11
- Muramatsu Y, Yoshida S (1995) Volatilization of methyl iodine from soil-plant system. *Atmos Environ* 29:21–25
- NSC (Nuclear Safety Commission) (2011) <http://www.nsc.go.jp/info/20110412.pdf>. Accessed Mar 2012
- ORNL (Oak Ridge National Laboratory) (2004) ORIGIN ARP 2
- Paatero J, Vira J, Siitari-Kauppi M, Hatakka J, Holmen K, Viisanen Y (2012) Airborne fission products in the high Arctic after the Fukushima nuclear accident. *J Environ Radioact* 114:41–47
- Pham MK, Eriksson M, Levy I, Nies H, Osvath I, Betti M (2012) Detection of Fukushima Daiichi nuclear power plant accident radioactive tracers in Monaco. *J Environ Radioact* 114:131–137
- Pittauerová D, Hettwig B, Fischer HW (2011) Fukushima fallout in Northwest German environmental media. *J Environ Radioact* 102:877–880

- RJG (Report of Japanese Government) (2011) The accident at TEPCO's Fukushima Nuclear Power 2011. http://www.kantei.go.jp/jp/Topics/2011/iaea_houkokusho.html. (Revised total release of radionuclides: <http://www.meti.go.jp/press/2011/10/20111020001.pdf>). Accessed Mar 2014
- Stohl A, Seibert R, Wotawa G, Arnold D, Burkhardt JF, Eckhardt S et al (2011) Xenon-133 and caesium-137 releases into the atmosphere from the Fukushima Dai-ichi nuclear power plant: determination of the source term, atmospheric dispersion, and deposition. *Atmos Chem Phys Discuss* 11:28319–28394
- Takemura T, Nakamura H, Takigawa M, Kondo H, Satomura T, Miyasaka T, Nakajima T (2011) A numerical simulation of global transport of atmospheric particles emitted from the Fukushima Daiichi Nuclear Power Plant. *Sora* 7:101–104
- TEPCO (Tokyo Electric Power Co.) (2011) Tentative estimation of atmospheric emission rate of radionuclides from the Fukushima Daiichi NPP. http://www.tepco.co.jp/cc/press/betsu11_j/images/107194.pdf. Accessed Mar 2012
- UNSCEAR (2000) Sources and effects of ionizing radiation, vol. 1: sources. United Nations, New York, pp 654
- Yonezawa C, Yamamoto Y (2011) Measurements of artificial radionuclides in surface air by CT-BTO network. *BUNSEKI* No. 8 pp 451–458 (In Japanese).
- Yoshida N, Takahashi Y (2012) Land-surface contamination by radionuclides from the Fukushima Daiichi Nuclear Power Plant accident. *Elements* 8:201–206
- Zhang W, Bean M, Benotto M, Cheung J, Ungar K, Ahier B (2011) Development of a new aerosol monitoring system and its application in Fukushima nuclear accident related aerosol radioactivity measurement at the CTBT radionuclide station in Sidney of Canada. *J Environ Radioact* 102:1065–1069